CCFE
CULHAM CENTRE FOR FUSION ENERGY

UK Atomic Energy Authority

UKAEA-CCFE-PR(18)38

Max Boleininger, Thomas D. Swinburne
and Sergei L. Dudarev

Atomistic-to-continuum description of edge dislocation core: unification of the Peierls-Nabarro model with linear elasticity

Atomistic-to-continuum description of edge dislocation core: unification of the Peierls-Nabarro model with linear elasticity

Max Boleininger,[a] Thomas D. Swinburne[b] and Sergei L. Dudarev[a]

[a]*CCFE, Culham Science Centre, UK Atomic Energy Authority, Abingdon, Oxfordshire OX14 3DB, United Kingdom*
[b]*Theoretical Division T-1, Los Alamos National Laboratory, Los Alamos, United States of America*

This is a preprint of a paper submitted for publication in Acta Materialia

Atomistic-to-continuum description of edge dislocation core: unification of the Peierls-Nabarro model with linear elasticity

Max Boleininger[a], Thomas D. Swinburne[b], and Sergei L. Dudarev[a]

[a]CCFE, Culham Science Centre, UK Atomic Energy Authority, Abingdon, Oxfordshire OX14 3DB, United Kingdom
[b]Theoretical Division T-1, Los Alamos National Laboratory, Los Alamos, United States of America

ARTICLE HISTORY
Compiled March 25, 2018

ABSTRACT
Conventional linear elasticity theory predicts the strain fields of a dislocation core to diverge, whereas it is known from atomistic simulations that strains at dislocation cores remain finite. We present an analytical solution to a generalised, variational Peierls-Nabarro model of edge dislocation displacement fields that features a finite core width, as well as the correct isotropic elastic behaviour at large distances away from the core. The strain fields are in qualitative agreement with atomistic simulations of $\frac{1}{2}[111](1\bar{2}1)$ edge dislocations in bcc tungsten and iron. The treatment is based on the Multi-String Frenkel-Kontorova model that we reformulate as a generalization of the Peierls-Nabarro model using the principle of least action.

KEYWORDS
Edge dislocation; dislocation core; isotropic linear elasticity; Frenkel-Kontorova; Peierls-Nabarro; tungsten; iron

1. Introduction

The assessment of accuracy of the line-tension model for modelling dislocations is essential for deriving physical models for dislocation energetics in dislocation dynamics simulations. Linear elasticity predicts that straight dislocations have negative line tension with respect to small fluctuations[1][2, ch. 6], suggesting that the energy of a dislocation would decrease as a result of it bowing out. This is in stark contrast to atomistic simulations that consistently predict positive line tension. The central problem of linear elasticity theory in this context is its inability to describe the displacement field of the dislocation core: the strain field of the dislocation is found to diverge in the glide-plane, leading to infinite energy density unless the divergence is cut out or otherwise regularised. A physically consistent treatment of the dislocation core is therefore a prerequisite for correctly describing dislocation line tension in a continuum model.

It was shown by Peierls[3] that the divergence can be resolved by the inclusion of a periodic misfit potential, representing the forces of the periodic arrangement of atoms in

CONTACT M. Boleininger. Email: max.boleininger@ukaea.uk
CONTACT T.D. Swinburne. Email: tomswinburne@gmail.com
CONTACT S.L. Dudarev. Email: sergei.dudarev@ukaea.uk

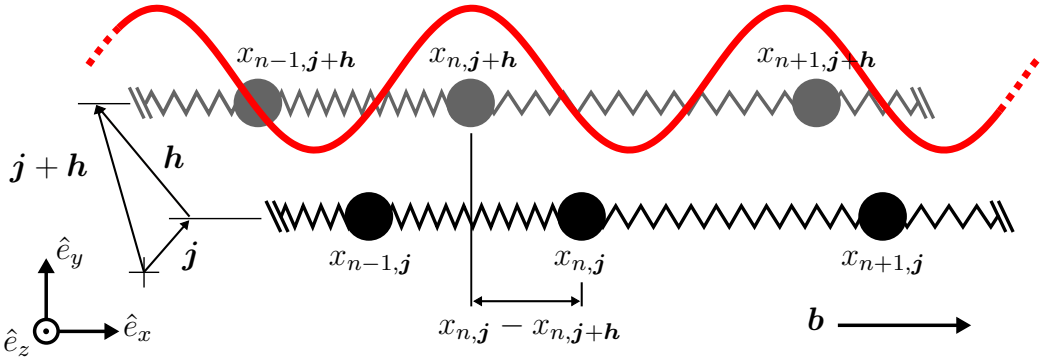

Figure 1. The Multi-String Frenkel-Kontorova model pictured in the xy-plane. Atoms in the lattice are classified by dividing the lattice into atomic strings lying parallel to the Burgers vector $\boldsymbol{b}$. Neighbouring atoms in a string interact harmonically. Each atom $x_{n,\boldsymbol{j}}$ interacts with the surrounding strings via a sinusoidal potential shifted by the displacement of a reference atom $x_{n,\boldsymbol{j}+\boldsymbol{h}}$.

the crystal lattice. The misfit potential energetically penalises concentrations of strain, causing the dislocation core to spread out and attain a finite size. Models developed later[4, ch.8][5,6] offer a connection between the generalised stacking fault energy and various phenomena involving dislocation cores. Yet a common drawback of these models is either an incomplete description of elasticity away from the core, or the lack of tractable analytical solutions.

We present a continuum theory of edge dislocation that features a finite core size, as in the Peierls-Nabarro[7] model, as well as displacements fields that are consistent with linear isotropic elasticity theory away from the core. The displacement fields are found to be in agreement with the atomistic displacements derived from molecular dynamics simulations of bcc iron and tungsten, provided that the dislocation core is wide enough to agree with the underlying continuum approximation. The model is derived from the discrete Multi-String Frenkel-Kontorova[8] (MSFK) model, which in the continuum limit unifies linear elasticity and the Peierls-Nabarro model in a consistent manner.

The derivation of the continuum equations from the MSFK model is outlined in section 2. The continuum model compatible with both the Peierls-Nabarro model and isotropic linear elasticity theory is presented and solved analytically in section 3 for a straight edge dislocation.

2. Analytical solution for the strain field of a straight edge dislocation

Atoms in the Multi-String Frenkel-Kontorova model are considered to interact harmonically with their nearest neighbours in the direction parallel to the Burgers vector, forming linear elastic strings. Each atom also feels the effect of sinusoidal potentials from the neighbouring strings, which may be locally shifted with respect to a reference string. To make an analytical solution possible, atoms are constrained to only move along the direction of the Burgers vector. Consequently the model only delivers the displacement field parallel to the Burgers vector of the dislocation.

Let the atomic positions $x_{n,\boldsymbol{j}}$ be indexed by their position n within a string, and by the vector-valued index $\boldsymbol{j}$ representing the string location in a plane orthogonal to the Burgers vector, as illustrated in Fig. 1. As the strings are parallel to the Burgers vector, in a monoatomic lattice the equilibrium atomic spacing along the string is the Burgers

vector length b. The discrete Lagrangian is expressed in terms of atomic displacements $u_{n,\boldsymbol{j}} = x_{n,\boldsymbol{j}} - nb$ as

$$\mathcal{L} = \sum_{\boldsymbol{j}} \sum_{n=-\infty}^{\infty} \left(\frac{m\dot{u}_{n,\boldsymbol{j}}^2}{2} - \frac{\alpha}{2} \left(u_{n+1,\boldsymbol{j}} - u_{n,\boldsymbol{j}} \right)^2 \right) - \frac{m\omega^2 b^2}{2\pi^2} \sum_{\boldsymbol{j},\boldsymbol{h}} \sum_{n=-\infty}^{\infty} \sin^2 \left(\frac{\pi}{b} (u_{n,\boldsymbol{j}} - u_{n,\boldsymbol{j}+\boldsymbol{h}}) \right), \tag{1}$$

where m is the atomic mass. For the edge-dislocation geometry considered here, the frequency ω characterizes the strength of interaction between the strings, and α characterizes the stiffness of harmonic interaction between neighbouring atoms in a string. Vector summation runs over the string positions $\boldsymbol{j}$ and the displacement vector $\boldsymbol{h}$ of their respective nearest neighbours.

We shall next introduce a dislocation into the material. For this purpose we divide $\mathbb{R}^3$ into two volumes, Ω^+ and Ω^-, separated by the dividing surface, $\partial\Omega$, as illustrated in Fig. 2. Note that the dividing surface must not cut through atomic strings; the surface normal is perpendicular to the string direction at any point in space, hence $n_x = 0$. The edge-dislocation is introduced as a discontinuity in the displacement boundary conditions as the dividing surface is crossed:

$$\begin{aligned} \lim_{n\to-\infty} u_{n,\boldsymbol{j}} &= \ \ b/2 \qquad \text{and} \quad \lim_{n\to\infty} u_{n,\boldsymbol{j}} = 0, \qquad \boldsymbol{j} \in \Omega^+, \\ \lim_{n\to-\infty} u_{n,\boldsymbol{j}} &= -b/2 \qquad \text{and} \quad \lim_{n\to\infty} u_{n,\boldsymbol{j}} = 0, \qquad \boldsymbol{j} \in \Omega^-, \end{aligned} \tag{2}$$

The dividing surface $\partial\Omega$ is therefore equivalent to the dislocation glide plane.

The Lagrangian (1) only depends on the difference between atomic displacements that are generally considered to vary slowly in space. An exception occurs when two neighbouring strings lie on opposite sides of the dividing surface due to the discontinuity introduced through the boundary conditions. The displacement field difference between strings within the same domain Ω^+ or Ω^- however is considered small, and the potential can therefore be linearised. The Lagrangian is split into three parts: two for the Ω^+ and Ω^- domains, and one for the dividing surface $\partial\Omega$, namely

$$\mathcal{L} = \mathcal{L}_{\Omega^+} + \mathcal{L}_{\Omega^-} + \mathcal{L}_{\partial\Omega}, \tag{3}$$

where:

$$\mathcal{L}_{\Omega^\pm} = \sum_{\boldsymbol{j}\in\Omega^\pm} \sum_{n=-\infty}^{\infty} \left(\frac{m\dot{u}_{n,\boldsymbol{j}}^2}{2} - \frac{\alpha}{2} \left(\frac{\partial u_{n,\boldsymbol{j}}}{\partial n} \right)^2 \right) - \frac{m\omega^2}{2} \sum_{\substack{\boldsymbol{j}\in\Omega^\pm \\ \boldsymbol{j}+\boldsymbol{h}\in\Omega^\pm}} \sum_{n=-\infty}^{\infty} \left(\frac{\partial u_{n,\boldsymbol{j}}}{\partial \boldsymbol{h}} \right)^2 \tag{4}$$

$$\mathcal{L}_{\partial\Omega} = -\frac{m\omega^2 b^2}{\pi^2} \sum_{\substack{\boldsymbol{j}\in\Omega^+ \\ \boldsymbol{j}+\boldsymbol{h}\in\Omega^-}} \sum_{n=-\infty}^{\infty} \sin^2 \left(\frac{\pi}{a} (u_{n,\boldsymbol{j}} - u_{n,\boldsymbol{j}+\boldsymbol{h}}) \right). \tag{5}$$

The summation in the surface term $\mathcal{L}_{\partial\Omega}$ runs over all the neighbouring string pairs on the opposing sides of the dividing surface. The factor of 2 compared to the original Lagrangian (1) is accounting for double-counting in the string summation.

In the continuum limit, the atomic displacements defined in $\Omega^\pm$, respectively, become continuous scalar fields $u^\pm = u^\pm(\boldsymbol{r}, t)$. The Lagrangian of the discrete system hence

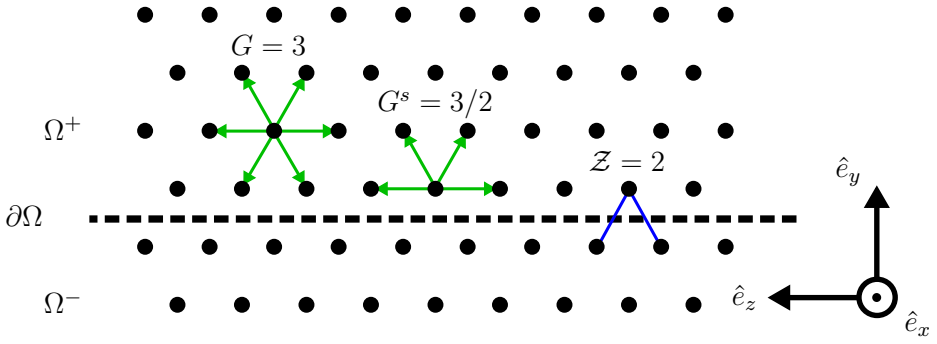

Figure 2. Continuum representation of the string summation terms for the example of a bcc $\frac{1}{2}[111](1\bar{2}1)$ edge dislocation, where $\boldsymbol{b} \parallel \hat{e}_x$. The black dots represent MSFK strings as seen in the direction parallel to the Burgers vector. Vectors shown in green illustrate summation over string-neighbour vectors $\boldsymbol{h}$. Note that summation is not performed across the glide plane $\partial\Omega$ (dashed line), leading to the structure constant G to adopt different values at the surface and in the bulk. The effective number of strings interacting across the plane in this example is $\mathcal{Z} = 2$.

becomes a volume integral over the Lagrange density:

$$\begin{aligned} L &= L_{\Omega^+} + L_{\Omega^-} + L_{\partial\Omega}, \\ L_{\Omega^\pm} &= \eta \int_{\Omega^\pm} \mathrm{d}V \left(\frac{m(\dot{u}^\pm)^2}{2} - \frac{\alpha b^2}{2} \left(\frac{\partial u^\pm}{\partial x} \right)^2 - \frac{m\omega^2 l^2}{2} {\sum_{\boldsymbol{h}}}' \left(\hat{e}^y_{\boldsymbol{h}} \frac{\partial u^\pm}{\partial y} + \hat{e}^z_{\boldsymbol{h}} \frac{\partial u^\pm}{\partial z} \right)^2 \right) \\ L_{\partial\Omega} &= \int_{\partial\Omega} \mathrm{d}S \left(-\mathcal{Z} \frac{m\omega^2 b}{\pi^2 l} \right) \sin^2 \left(\frac{\pi}{b}(u^+ - u^-) \right), \end{aligned} \tag{6}$$

where η is the atom number density, l is the perpendicular distance between neighbouring strings, $\hat{e}^y_{\boldsymbol{h}} = \hat{e}_y.\boldsymbol{h}/\|\boldsymbol{h}\|$, and $\mathcal{Z}$ refers to the effective number of neighbouring strings that lie across the dividing surface. The displacement fields on the dividing surface are defined in terms of the limit approaching the surface, namely

$$u^\pm(\boldsymbol{r}) = \lim_{\gamma \to 0^\pm} u^\pm(\boldsymbol{r} - \gamma \boldsymbol{n}^\pm(\boldsymbol{r})), \qquad \boldsymbol{r} \in \partial\Omega \tag{7}$$

where $\boldsymbol{n}^\pm(\boldsymbol{r})$ are the outwards-facing surface normals of the domains $\Omega^\pm$, hence $\boldsymbol{n}^+(\boldsymbol{r}) = -\boldsymbol{n}^-(\boldsymbol{r})$.

Some subtleties are involved in taking the continuum limit. Consider the second term in equation (4). The string summation is performed in such a way that only strings within the same domain Ω^+ or Ω^- interact; the interaction does not cross the glide plane $\partial\Omega$. Summation over the neighbouring strings $\boldsymbol{h}$ in equation (6) therefore leaves out the strings lying across the glide plane $\partial\Omega$ if integration is performed over the surface, which is indicated by the primed summation symbol. We refer to figure 2 for a visual guide.

We proceed by minimising the action associated with the Lagrangian with respect to variation in displacement fields and their derivatives, arriving at the MSFK equations

of motion:

$$
\begin{aligned}
0 &= -\ddot{u}^+ + c^2 u^+_{xx} + \omega^2 l^2 G(u^+_{yy} + u^+_{zz}), && \boldsymbol{r} \in \Omega^+ \\
0 &= -\ddot{u}^- + c^2 u^-_{xx} + \omega^2 l^2 G(u^-_{yy} + u^-_{zz}), && \boldsymbol{r} \in \Omega^- \\
0 &= G^s_{yy} u^+_y n^+_y + G^s_{zz} u^+_z n^+_z + 2G^s_{yz}(n^+_y u^+_z + n^+_z u^+_y) + \frac{\mathcal{Z}}{\pi\eta l^3} \sin\left(\frac{2\pi}{b}(u^+ - u^-)\right), && \boldsymbol{r} \in \partial\Omega \\
0 &= G^s_{yy} u^-_y n^-_y + G^s_{zz} u^-_z n^-_z + 2G^s_{yz}(n^-_y u^-_z + n^-_z u^-_y) - \frac{\mathcal{Z}}{\pi\eta l^3} \sin\left(\frac{2\pi}{b}(u^+ - u^-)\right), && \boldsymbol{r} \in \partial\Omega,
\end{aligned}
\tag{8}
$$

where $\alpha b^2/m = c^2$, and $u_i = \partial u/\partial i$. The structure constant G_{ij} is defined as $G_{ij} = \sum'_{\boldsymbol{h}} \hat{e}^i_{\boldsymbol{h}} \hat{e}^j_{\boldsymbol{h}}$, and equals $G_{ij} = G\delta_{ij}$ in the bulk, where $G = 2$ for the square lattice and $G = 3$ for the hexagonal lattice. The value of constant G^s_{ij} in the glide plane depends on the geometry of the dislocation cut, as lattice vectors $\boldsymbol{h}$ crossing the glide plane are left out of the summation. Note that we have used condition $n^\pm_x = 0$.

We shall next restrict ourselves to the treatment of a straight edge dislocation, by aligning the dividing surface with the xz-plane. Domains $\Omega^\pm$ now become the upper and lower open half-planes in $\mathbb{R}^2$, respectively

$$
\begin{aligned}
\Omega^+ &= \{(x,\ y) \in \mathbb{R}^2 \mid y > 0\} \\
\Omega^- &= \{(x,\ y) \in \mathbb{R}^2 \mid y < 0\} \\
\partial\Omega\ &= \{(x,\ y) \in \mathbb{R}^2 \mid y = 0\},
\end{aligned}
\tag{9}
$$

with the normal vector components of $n^\pm_y = \mp 1$ and $n^\pm_z = 0$. The z-coordinate can be left out as the edge-dislocation strain fields are translationally invariant along the line-direction $\hat{e}_z$, hence $u^\pm_z = u^\pm_{zz} = 0$. We further consider the dislocation to be static, $\ddot{u}^\pm = 0$, to arrive at the elastostatic equations. Equations of motion now reduce to a boundary value problem:

$$
u^+_{xx} + \frac{\omega^2 l^2 G}{c^2} u^+_{yy} = 0, \qquad y > 0 \tag{10}
$$

$$
u^-_{xx} + \frac{\omega^2 l^2 G}{c^2} u^-_{yy} = 0, \qquad y < 0 \tag{11}
$$

$$
\frac{\pi\eta l^3 G^s}{\mathcal{Z}} u^+_y = \frac{\pi\eta l^3 G^s}{\mathcal{Z}} u^-_y = \sin\left(\frac{2\pi}{b}(u^+ - u^-)\right), \qquad y = 0, \tag{12}
$$

where $G^s = G^s_{yy}$. This boundary value problem is reminiscent of Peierls' formalism[3], although the MSFK equations of motion have a more general range of validity and span the entire space $\mathbb{R}^2$.

At this point we can also establish a connection between the non-singular MSFK model and the isotropic elastostatic equations. The elastostatic equations follow from Hooke's law, $\sigma_{ij} = \sum_{kl} c_{ijkl}(u_{k,l} + u_{l,k})/2$, the stationary stress condition, $\sum_j \sigma_{ij,j} = 0$, and plane-strain conditions, $u_z = 0$:

$$
\begin{aligned}
u_{x,xx} + \frac{1-2\nu}{2(1-\nu)} u_{x,yy} &= -\frac{1}{2(1-\nu)} u_{y,xy} \\
u_{y,yy} + \frac{1-2\nu}{2(1-\nu)} u_{y,xx} &= -\frac{1}{2(1-\nu)} u_{x,yx}
\end{aligned}
\tag{13}
$$

The elastostatic equations can be matched to MSFK by restricting the displacements to only occur in the u_x direction:

$$u_{x,xx} + \frac{1-2\nu}{2(1-\nu)} u_{x,yy} = 0 \tag{14}$$

From this comparison we identify the MSFK constants $\frac{\omega^2 l^2 G}{c^2}$ as $\frac{1-2\nu}{2(1-\nu)}$, leading to the MSFK definition of Poisson's ratio:

$$\nu = \frac{\alpha b^2 - 2Gl^2 m\omega^2}{2(\alpha b^2 - Gl^2 m\omega^2)}. \tag{15}$$

This result has a clear meaning. We see that the ratio of deformations along x and y is intrinsically related to the interatomic interaction strengths along those directions, respectively proportional to α and $m\omega^2$, and the interatomic spacing, respectively given by b and l.

We now need to solve the problem posed by equations (10)-(12). The solution is easily found if we know that the displacement field is mirrored with respect to the $x = 0$ axis: $u^+(x, y) = -u^-(x, -y)$. While this can be motivated by our knowledge of the analytical displacement field of a Volterra edge-dislocation, the proof involving equations (10)-(12) is more elaborate. Assuming $u^+(x, y) = -u^-(x, -y)$, we only need to consider the boundary value problem in the upper half-plane:

$$\begin{aligned} u^+_{xx} + \frac{1-2\nu}{2(1-\nu)} u^+_{yy} &= 0, \quad y > 0 \\ \frac{4\pi}{p} u^+_y &= \sin\left(\frac{4\pi}{b} u^+\right), \quad y = 0, \end{aligned} \tag{16}$$

where $p = \mathcal{Z}/(\eta l^3 G^s)$ is the dimensionless surface structure constant. The solution to the problem above, after some minor substitutions, has been found by Dudarev[8], namely

$$\begin{aligned} u^+(x, y) &= \frac{b}{2\pi}\left(\frac{\pi}{2} - \arctan\left(\frac{px}{b + py}\sqrt{\frac{1-2\nu}{2(1-\nu)}}\right)\right), \quad y > 0 \\ u^-(x, y) &= \frac{b}{2\pi}\left(\frac{\pi}{2} + \arctan\left(\frac{px}{b - py}\sqrt{\frac{1-2\nu}{2(1-\nu)}}\right)\right), \quad y < 0, \end{aligned} \tag{17}$$

or

$$u(x, y) = \frac{b}{2\pi}\left(\frac{\pi}{2} - \mathrm{sgn}(y)\arctan\left(\frac{px}{b + p|y|}\sqrt{\frac{1-2\nu}{2(1-\nu)}}\right)\right), \quad y \in \mathbb{R}\backslash\{0\}, \tag{18}$$

where sgn is the sign-function: $\mathrm{sgn}(x) = 1$ if $x > 0$, otherwise -1.

A useful measure for the dislocation core width w is the full-width at half-maximum of the $\partial u(x, y)/\partial x$ strain-field in the glide plane, that is for $y \to 0$:

$$w = \frac{b}{p}\sqrt{\frac{2(1-\nu)}{1-2\nu}} \tag{19}$$

The key feature of this solution is that the core width w remains finite as predicted by atomistic simulations; the strain-field $\partial u(x,y)/\partial x$ does not diverge on the glide-plane. Another interesting finding is that the dimensionless surface-structure constant $p = \mathcal{Z}/(\eta l^3 G^s)$ controlling the core width is solely determined by the crystal structure and the geometry of the edge-dislocation cut. This suggests that the width of the dislocation core does not depend on the details of the chosen interatomic potential.

We have so far neglected the displacement field perpendicular to the Burgers vector. This is evident in the simplification of the elastostatic equation (13) to (14).

3. Analytical solution for the full strain field of an edge dislocation

It appears possible to extend the MSFK model into two dimensions by including the appropriate interactions between the atomic strings in the directions perpendicular to the Burgers vector. The detailed nature of such interactions is not of major interest as there is in principle an endless variety of interatomic potentials that all reproduce the elastostatic equations. We present one such example of a minimal two-dimensional discrete MSFK model in the appendix.

The two-dimensional MSKF model offers a physically motivated extension of the Peierls original description of the edge dislocation core, valid in the entire space and consistent with isotropic linear elasticity. The surface boundary value problem is unchanged by the presence of the transverse field u_y. We are hence justified in using a generalized elastostatic boundary value problem in two dimensions:

$$\begin{aligned}
&u^+_{x,xx} + \frac{1-2\nu}{2(1-\nu)} u^+_{x,yy} = -\frac{1}{2(1-\nu)} u^+_{y,xy} \qquad y>0 \\
&u^+_{y,yy} + \frac{1-2\nu}{2(1-\nu)} u^+_{y,xx} = -\frac{1}{2(1-\nu)} u^+_{x,yx} \qquad y>0 \\
&\frac{2(1-\nu)}{3-2\nu} \lim_{y\to 0^+} \frac{4\pi}{p} u^+_{x,y} = \lim_{y\to 0^+} \sin\left(\frac{4\pi}{b} u^+_x\right),
\end{aligned} \tag{20}$$

where we have re-scaled the surface-structure constant p to make the solution more readable:

$$p \equiv \frac{\mathcal{Z}}{\eta l^3 G^s} \cdot \frac{3-2\nu}{2(1-\nu)}. \tag{21}$$

The boundary value problem (20) can be solved by making an educated guess. We have found the following solution:

$$\begin{aligned}
u_x &= \frac{b\ \mathrm{sgn}(y)}{2\pi}\left(\frac{\pi}{2} + \frac{1}{2(1-\nu)}\frac{p^2 x|y|}{(px)^2 + (p|y|+b)^2} - \arctan\left(\frac{px}{p|y|+b}\right)\right) \\
u_y &= \frac{b}{8\pi(1-\nu)}\left(\frac{2p|y|(b+p|y|)}{(px)^2+(p|y|+b)^2} - (1-2\nu)\ln\left(\frac{(px)^2+(p|y|+b)^2}{p^2}\right) - 1\right)
\end{aligned} \tag{22}$$

Substituting the above equations into the boundary value problem (20) confirms the validity of this solution. It is evident that the solution reduces to the analytical form of

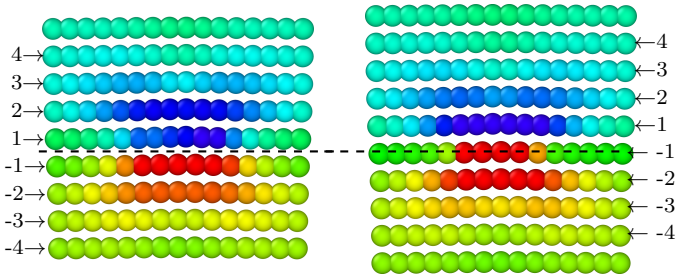

(a) symmetrical (b) asymmetrical

Figure 3. Atomistic strain fields $u_{x,x}$ for the tungsten $\frac{1}{2}[111](1\bar{2}1)$ edge dislocation core. Two repeating configurations are found along the dislocation line direction: a symmetric (a) and an asymmetric (b). Blue colour corresponds to the compressive strain and red colour to the tensile strain. The first few atomic rows above and below the glide-plane (black, dashed line) are indexed as shown in the figure.

the Volterra edge dislocation[2] in the $p \to \infty$ limit:

$$\begin{aligned} \lim_{p\to\infty} u_x = u_x^{\text{Volterra}} &= \frac{b}{2\pi}\left(\operatorname{sgn}(y)\frac{\pi}{2} + \frac{1}{2(1-\nu)}\frac{xy}{x^2+y^2} - \arctan\left(\frac{x}{y}\right)\right) \\ \lim_{p\to\infty} u_y = u_y^{\text{Volterra}} &= \frac{b}{8\pi(1-\nu)}\left(\frac{y^2-x^2}{x^2+y^2} - (1-2\nu)\ln\left(x^2+y^2\right)\right). \end{aligned} \tag{23}$$

We now benchmark the model with the reference data derived from atomistic simulations.

4. Atomistic setup

Atomistic simulations were performed using LAMMPS[9] for iron and tungsten, for two different interatomic potentials for each material. The simulation cell was initialised as a pristine bcc lattice with the coordinate system aligned along $x = [111]$, $z = [1\bar{2}1]$, and $y = [\bar{1}01]$. The crystal lattice fills a volume of $120 \times 120 \times 6$ lattice units with periodic boundary conditions applied to the line-direction $z = [1\bar{2}1]$. A dislocation was introduced by applying anisotropic linear-elastic displacement field of the $\frac{1}{2}[111](1\bar{2}1)$ edge-dislocation at the box centre, using elastic constants appropriate for the chosen interatomic potential. Atomic coordinates were relaxed while keeping atoms beyond a distance of 100 lattice units from the dislocation line fixed at positions corresponding to a solution in an infinite elastic medium. Atomistic strain and displacement fields were computed in reference to the perfect bcc structure.

Two alternating atomic configurations are found along the $[1\bar{2}1]$ line direction, see figure 3. The $u_{x,x}$ strain field in one of the configurations is strongly asymmetric at the core, as the apparent height of the glide plane is not centred between the atomic rows. Our comparison of atomistic and continuum strain fields is therefore solely focused on the symmetric configuration.

The surface structure constant p for each case is found by fitting the $u_{x,x}$ component of the continuum strain field to the atomistic strain fields at the position of two atomic rows above and below the glide plane. We refer to table 1 for a comparison of the fitted constants to their MSFK value as determined by the crystal structure (21). The fitted values for p are found to vary little between the various potentials. The value of the

constant does not depend on the details of the interatomic potentials, though that is only true within the approximations inherent to MSFK. It is therefore not surprising that atomistic simulations show small variation of the surface structure constant even for the same dislocation geometry.

Table 1. Surface-structure constant p as fitted for tungsten and iron and as computed from MSFK (21). The dislocation width $w(p)$ is computed in the glide plane according to the MSFK model.

material	model	p	$w(p)/b$
W	Marinica *et al.*[10]	0.81	2.48
	Mason *et al.*[11]	1.00	2.00
Fe	Ackland *et al.*[12]	0.83	2.41
	Gordon *et al.*[13]	0.98	2.04
-	MSFK[a]	1.11	1.79

[a]for Poisson's ratio $\nu = 0.28$, $G^s = 3/2$ (see fig. 2)

A comparison of the continuum and atomistic strain fields for tungsten computed using the Marinica *et al.*[10] EAM4 potential is shown in figure 4. The MSFK and atomistic strain fields for tungsten are in good agreement everywhere in space. The strain fields for iron, see the supplemental material, deviate slightly for larger distances from the core. Iron exhibits considerable elastic anisotropy and therefore requires an anisotropic linearly elastic model.

The magnitude of the atomistic tensile strain is generally higher than the atomistic compressive strain. Several phenomena can affect the symmetry of the strain fields. For instance, the glide-plane may not be evenly centred between the atomic rows, which is the case for configuration (b) in figure 3. Another explanation is that in many empirical potentials it takes more energy to compress atoms than to stretch them, hence tensile strains will be larger than compressive strains under equal stress.

We have also repeated the same procedure for the [100](010) edge dislocation that has a comparatively narrow core width. This is reflected in the MSFK surface structure constant p acquiring the value of 4.72. The MSFK model is unable to match the atomistic strain fields, as these are more localized than what is permitted by the Volterra solution in the limit $p \to \infty$. The atomistic strain fields for the [100](010) configuration vary strongly on the scale of interatomic lattice spacing, hence it can be reasoned that the continuum approximation inherent to the MSFK model becomes invalid.

5. Peierls migration barrier

There is no energy barrier associated with dislocation glide in the continuum model, as the displacement fields are translationally invariant in the direction of the Burgers vector. In an atomic lattice however, the displacement fields are resolved discretely on lattice sites, consequently the total elastic energy per dislocation length L varies periodically as a function of the displacement field centre (x_0, y_0). The exact analytical solution of the displacement fields in the 2D-MSFK model enables us to estimate the barrier with little computational effort.

The dislocation glide is considered to proceed along the minimum energy pathway, defined as the trajectory connecting the global energy minima corresponding to the adjacent periodic cells with the smallest possible energy barrier. This energy barrier

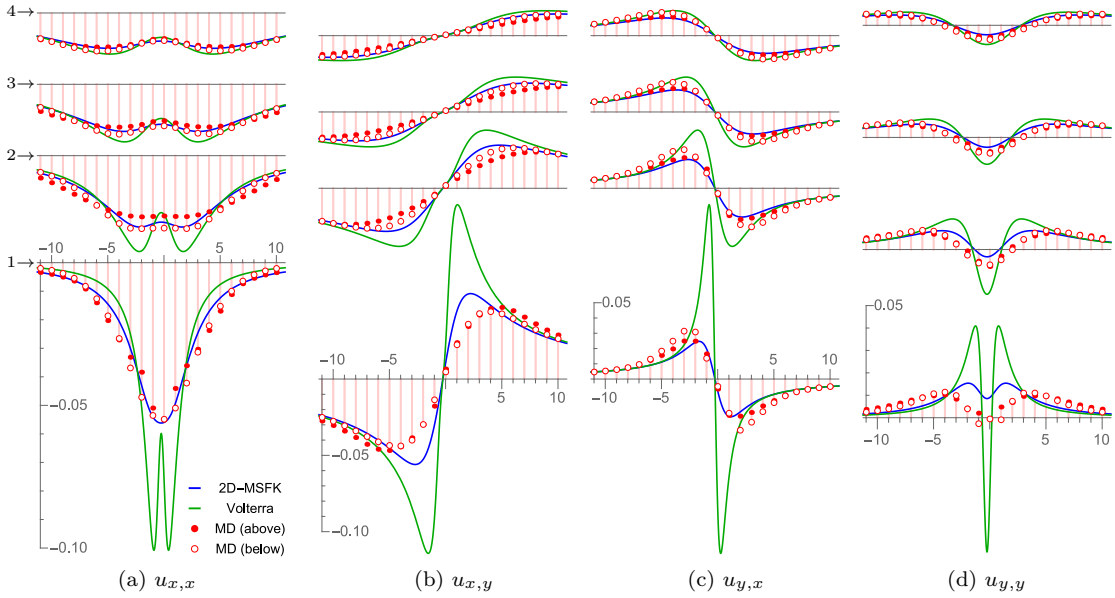

(a) $u_{x,x}$ (b) $u_{x,y}$ (c) $u_{y,x}$ (d) $u_{y,y}$

Figure 4. Strain fields in the vicinity of $\frac{1}{2}[111](1\bar{2}1)$ edge dislocation core in tungsten. The strain fields at the first four atomic rows above (compressive strain, filled dots) and below (tensile strain, unfilled dots) the glide-plane are pictured here, according to the indices in figure 3. The x-axis is given in units of the Burgers vector length b, and the y-axis refers to the dimensionless strains $u_{i,j}$. Graphs for the same strain use identical axes scales, and the tensile strains pictured here are point-reflected.

is commonly referred to as the Peierls migration barrier[3]. We compute the barrier by evaluating the discrete expressions for the dislocation energy using the continuum solution[1] for the displacement fields u_x and u_y as shown in Eq. (23).

The migration pathway is approximated to lie along the fixed height $y_0 = y_{\min}$ where the energy minimum $(x_{\min},\ y_{\min})$ of the bulk energy $\mathcal{L}_{\text{bulk}}(x_0,\ y_0)$ occurs[2]. The Peierls barrier is then given by:

$$\mathcal{L}_{\text{net}}(x_0,\ y_0) = \mathcal{L}_{\text{bulk}}(x_0,\ y_0) + \mathcal{L}_{\partial\Omega}(x_0,\ y_0) \tag{24}$$

$$V_P = \left(\max_{x_0\in[0,b)}\mathcal{L}_{\text{net}}(x_0,\ y_{min}) - \min_{x_0\in[0,b)}\mathcal{L}_{\text{net}}(x_0,\ y_{min})\right)/L. \tag{25}$$

We express the shear modulus μ in terms of the MSFK force constants by comparing the MSFK equation of motion with the elastostatic equation (before cancelling constants):

$$\mu = m\omega^2 l^2 \eta G. \tag{26}$$

Let $x_{n,\boldsymbol{j}}$, $y_{n,\boldsymbol{j}}$, and $z_{n,\boldsymbol{j}}$ be the coordinates of the pristine, unstrained lattice. The inter-

[1]The continuum solution can be used for a discrete lattice if the displacement fields vary slowly in comparison to the atomic spacings. Hence we expect greater uncertainties for the [100](010) configuration.

[2]The bulk energy $\mathcal{L}_{\text{bulk}}$ diverges with respect to system size, while the interfacial energy $\mathcal{L}_{\partial\Omega}$ remains finite. The change in bulk energy for dislocation translation however is finite. Consequently, the energy barrier is a well-defined finite quantity and the migration pathway passes through energy minima of the bulk energy.

facial energy (5) is expressed as:

$$\mathcal{L}_{\partial\Omega}(x_0, y_0) = -\frac{\mu b^2}{\pi^2 l^2 \eta G} \sum_{\substack{\boldsymbol{j}\in\Omega^+ \\ \boldsymbol{j}+\boldsymbol{h}\in\Omega^-}} \sum_{n=-\infty}^{\infty} \sin^2\left(\frac{\pi}{b}((u_x)_{n,\boldsymbol{j}} - (u_x)_{n,\boldsymbol{j}+\boldsymbol{h}})\right). \tag{27}$$

where $(u_i)_{n,\boldsymbol{j}} = u_i(x_{n,\boldsymbol{j}} - x_0, y_{n,\boldsymbol{j}} - y_0)$ represents the displacement field in i-direction according to the continuum solution (23), offset by the dislocation centre $(x_0,\ y_0)$. The bulk energy is expressed in terms of the standard isotropic elastic energy evaluated at the discrete lattice coordinates:

$$\mathcal{L}_{\text{bulk}}(x_0, y_0) = -\frac{1}{2\eta} \sum_{\boldsymbol{j}\in\mathbb{R}^3} \sum_{n=-\infty}^{\infty} \sum_{ipkl} c_{ipkl}(\varepsilon_{ip})_{n,\boldsymbol{j}}(\varepsilon_{kl})_{n,\boldsymbol{j}}, \tag{28}$$

where c_{ipkl} is the isotropic stiffness tensor, η is the atom number density, and $(\varepsilon_{ip})_{n,\boldsymbol{j}}$ is the strain tensor:

$$(\varepsilon_{ip})_{n,\boldsymbol{j}} = \frac{1}{2}\left((u_{i,p})_{n,\boldsymbol{j}} + (u_{p,i})_{n,\boldsymbol{j}}\right). \tag{29}$$

The total energy (24) is evaluated numerically for the tungsten edge dislocations, using the structure constants appropriate to the $\frac{1}{2}[111](1\bar{2}1)$ and $[100](010)$ orientations, as shown in table 2. The Peierls barrier in the atomistic reference is obtained by migrating one dislocation in a dipole pair using the nudged elastic band method[14], subsequently correcting the energy for elastic interactions. The $\frac{1}{2}[111](1\bar{2}1)$ and $[100](010)$ dislocations have a migration period of $b/3$ and b respectively.

Table 2. Peierls barrier V_P for the tungsten $\frac{1}{2}[111](1\bar{2}1)$ and $[100](010)$ edge dislocations computed using appropriate parameters for tungsten ($\mu = 160\,\text{GPa}$, $\nu = 0.28$).

type	p	$V_P^{\text{MSFK}}/\text{meV Å}^{-1}$	$V_P^{\text{MD}}/\text{meV Å}^{-1}$
$\frac{1}{2}[111](1\bar{2}1)$	1.11	$< 10^{-4}$	0.918
$[100](010)$	4.72	143	274

The MSFK and MD barriers for the $[100](010)$ dislocation are found to be similar. The $\frac{1}{2}[111](1\bar{2}1)$ barrier is considerably lower in MD, however in the MSFK model it vanishes almost entirely due to a combination of wide core width and staggered atomic stacking in the $(1\bar{2}1)$ direction. We considered the continuum displacement fields as identical for every atomic layer in the $(1\bar{2}1)$ direction, effectively neglecting core interactions between atomic layers. More sophisticated models based on Peierls-Nabarro can attain migration barriers quantitatively comparable to those found in atomistic simulations[15–17].

6. Conclusion

In this treatise, we have systematically derived and validated a continuum non-singular model that predicts strain fields of an edge dislocation, including its core. Predictions derived from the model are consistent with atomistic simulations performed using several interatomic potentials, for the $\frac{1}{2}[111](1\bar{2}1)$ edge dislocation in iron and tungsten. Analytical solutions found for the edge dislocation strain fields are explicit and exact.

The model provides a physically motivated connection between equations of linear elasticity and the Peierls-Nabarro boundary value problem. Although the model is in principle parameter free, the surface structure constant p offers a convenient way of controlling the dislocation core width. For wider dislocation cores the constant p can be fitted to reproduce atomistic strain fields, while for narrow dislocation cores some alternative measures, such as line-tension, need to be considered due to the limitations inherent to the continuum approximation.

Further work can be well motivated by applying the model to more complex systems, such as screw and mixed dislocations, interacting dislocation segments, and most importantly line tension calculations for curved dislocation. The availability of reference data from atomistic simulations offers a promising testing ground for these applications.

Acknowledgements

Useful conversations with Jacob Chapman and Andrew London are gratefully acknowledged.

Disclosure statement

No potential conflict of interest is reported by the authors.

Funding

This work has been carried out within the framework of the EUROfusion Consortium and has received funding from the Euratom research and training programme 2014-2018 under Grant Agreements No. 633053 and No. 755039. Also, it has been partially funded by the RCUK Energy Programme (Grant No. EP/P012450/1). The views and opinions expressed herein do not necessarily reflect those of the European Commission.

References

[1] Szajewski B, Pavia F, Curtin W. Robust atomistic calculation of dislocation line tension. Modelling and Simulation in Materials Science and Engineering. 2015;23(8):085008.
[2] Anderson P, Hirth J, Lothe J. Theory of dislocations. Cambridge University Press; 2017.
[3] Peierls R. The size of a dislocation. Proceedings of the Physical Society. 1940;52(1):34.
[4] Bulatov V, Cai W. Computer simulations of dislocations. Vol. 3. Oxford University Press; 2006.
[5] Lu G. The Peierls-Nabarro model of dislocations: a venerable theory and its current development. In: Handbook of materials modeling. Springer; 2005. p. 793–811.
[6] Schoeck G. The peierls model: progress and limitations. Materials Science and Engineering: A. 2005;400:7–17.
[7] Nabarro F. Dislocations in a simple cubic lattice. Proceedings of the Physical Society. 1947;59(2):256.
[8] Dudarev S. Coherent motion of interstitial defects in a crystalline material. Philosophical Magazine. 2003;83(31-34):3577–3597.
[9] Plimpton S. Fast parallel algorithms for short-range molecular dynamics. Journal of computational physics. 1995;117(1):1–19.

[10] Marinica MC, Ventelon L, Gilbert M, et al. Interatomic potentials for modelling radiation defects and dislocations in tungsten. Journal of Physics: Condensed Matter. 2013; 25(39):395502.
[11] Mason D, Nguyen-Manh D, Becquart C. An empirical potential for simulating vacancy clusters in tungsten. Journal of Physics: Condensed Matter. 2017;29(50):505501.
[12] Ackland G, Bacon D, Calder A, et al. Computer simulation of point defect properties in dilute Fe-Cu alloy using a many-body interatomic potential. Philosophical Magazine A. 1997;75(3):713–732.
[13] Gordon P, Neeraj T, Mendelev M. Screw dislocation mobility in bcc metals: a refined potential description for α-Fe. Philosophical Magazine. 2011;91(30):3931–3945.
[14] Henkelman G, Uberuaga BP, Jónsson H. A climbing image nudged elastic band method for finding saddle points and minimum energy paths. The Journal of chemical physics. 2000;113(22):9901–9904.
[15] Wei H, Xiang Y, Ming P. A generalized Peierls-Nabarro model for curved dislocations using discrete Fourier transform. Communications in computational physics. 2008;4(2):275–293.
[16] Kang K, Bulatov VV, Cai W. Singular orientations and faceted motion of dislocations in body-centered cubic crystals. Proceedings of the National Academy of Sciences. 2012; 109(38):15174–15178.
[17] Liu G, Cheng X, Wang J, et al. Atomically informed nonlocal semi-discrete variational Peierls-Nabarro model for planar core dislocations. Scientific Reports. 2017;7:43785.

Appendix A. The two-dimensional Multi-String Frenkel-Kontorova model

In the one-dimensional MSFK model we consider atoms to interact harmonically with their nearest neighbours in direction of the Burgers vector. The first step is to also consider atoms to interact harmonically to their nearest neighbours in the perpendicular direction, with neighbouring strings interacting through a sinusoidal potential. If we let $\boldsymbol{b} \parallel \hat{e}_x$ and $\boldsymbol{b} \perp \hat{e}_y$, assuming plane-strain conditions in z-direction, we obtain an additional equation of motion for the transversal field u_y:

$$u_{y,yy} + \frac{\omega^2 l^2 G}{c^2} u_{y,xx} = 0 \tag{A1}$$

We have chosen the stiffness and string-interaction strength such that identical prefactors as for the u_x field are obtained, as required by the isotropic elasticity. We do not need to split the transversal field between upper and lower domains $\Omega^{\pm}$ because edge dislocation discontinuity only applies to the boundary conditions of u_x. A comparison with the elastostatic equations (13) makes clear that we need to further add coupling between fields u_x and u_y.

For the sake of simplicity, we shall restrict the discussion that follows to atoms arranged in a two-dimensional square lattice with a spacing of b. The displacement fields of an atom originally placed at $\boldsymbol{r}_{n,m} = nb\hat{e}_x + mb\hat{e}_y$ are written as $u^x_{n,m}$ and $u^y_{n,m}$. We add a cross coupling term to the discrete Lagrangian:

$$\mathcal{L}_{xy} = \sum_{\substack{n,m \\ n'=\pm 1 \\ m'=\pm 1}} n'm'V_0 \sin\left(\frac{\pi}{b}(u^x_{n+n',m+m'} - u^x_{n,m})\right) \sin\left(\frac{\pi}{b}(u^y_{n+n',m+m'} - u^y_{n,m})\right). \tag{A2}$$

Approximating the displacement differences to first order according to

$$u^i_{n\pm1,m\pm1} = u^i_{n,m} \pm b\frac{\partial u^i_{n,m}}{\partial n} \pm b\frac{\partial u^i_{n,m}}{\partial m}, \tag{A3}$$

the Lagrangian is linearised in the continuum limit:

$$L_{xy} = \eta \int \mathrm{d}V \; 4\pi^2 V_0 \left(u_{x,x}u_{y,y} + u_{x,y}u_{y,x}\right). \tag{A4}$$

Using the principle of least action we see that the coupling Lagrangian contributes mixed terms to the equations of motion:

$$\begin{aligned} u^{\pm}_{x,xx} + \frac{\omega^2 l^2 G}{c^2} u^{\pm}_{x,yy} + 4\pi^2 V_0 u_{y,xy} &= 0 \\ u_{y,yy} + \frac{\omega^2 l^2 G}{c^2} u_{y,xx} + 4\pi^2 V_0 u^{\pm}_{x,xy} &= 0. \end{aligned} \tag{A5}$$

We are free to choose the coupling-potential strength V_0 such that the correct form for linear elasticity is obtained:

$$4\pi^2 V_0 = \frac{1}{2(1-\nu)} = \frac{\omega^2 l^2 G}{c^2} - 1, \tag{A6}$$

where the MSFK definition of Poisson's ratio (15) was used. This leads to the elastostatic equations:

$$\begin{aligned} u^{\pm}_{x,xx} + \frac{1-2\nu}{2(1-\nu)} u^{\pm}_{x,yy} &= -\frac{1}{2(1-\nu)} u_{y,xy} \\ u_{y,yy} + \frac{1-2\nu}{2(1-\nu)} u_{y,xx} &= -\frac{1}{2(1-\nu)} u^{\pm}_{x,xy}. \end{aligned} \tag{A7}$$

In summary, we have derived the elastostatic equations from a two-dimensional discrete Multi-String Frenkel-Kontorova model for a simple cubic crystal structure.

It remains to characterise the influence of the cross-coupling Lagrangian on the boundary value problem. Similarly to the 1D-MSFK case, we consider strings lying on opposing sides of the dividing surface:

$$\mathcal{L}_{xy,\partial\Omega} = -2 \sum_{\substack{n,m \\ n'=\pm1}} n' V_0 \sin\left(\frac{\pi}{b}(u^x_{n+n',m-1} - u^x_{n,m})\right) \sin\left(\frac{\pi}{b}(u^y_{n+n',m-1} - u^y_{n,m})\right). \tag{A8}$$

Exploiting the symmetries of the straight edge dislocation displacement fields as known from the linear elasticity solution, we arrive at the interfacial Lagrangian in the continuum limit:

$$L_{xy,\partial\Omega} = \frac{4V_0}{b^2} \int_{\partial\Omega} \mathrm{d}S \; \cos\left(\pi u^-_{x,x}\right) \sin\left(\frac{2\pi}{b} u^+_x\right) \sin(\pi u_{y,x}). \tag{A9}$$

The interfacial Lagrangian vanishes because $u_{y,x}$ is an odd function with respect to x. For generally curved dislocations that is not the case; neglecting the effect of transverse

fields on the boundary value problem is equivalent to the planar core approximation commonly used in Peierls-Nabarro models.

The derivation for a more general crystal lattice follows equivalently, but the notation is opaque as we would be handling two separate sets of string vectors, displacement vectors, and string distances.